DRAFT

14053

Basalt

251.32 grams

Figure 1: PET photo of top surface of 14053 showing micrometeorite craters. Cube is 1 inch high. NASA photo # S71-35849.

Introduction

14053 is an Al-rich mare basalt found perched on the side of a boulder at station C2 (see figure 55 in Swann et al. 1977). It is flat with one side (freshly broken) with the other side rounded and pitted by microcraters (figure 1). Breccia material was found attached to flat side, indicating that this basalt was a clast in the boulder (breccia).

This basalt from Apollo 14 was found to have low siderophile content leading to the interpretation that it was yet another important type of mare basalt (also found as clasts in the Apollo 14 soil and breccia samples). The age determined for 14053 indicates that it is older than the Fra Mauro Formation.

A review of non-mare basalts is found in Irving (1975).

Petrography

LSPET (1971) and Gancarz et al. (1971) describe 14053 as an ophitic basalt with large, zoned, pyroxene grains surrounding laths of plagioclase (figure 2). Papike et al. (1976) describe 14053 as a medium-grained microgabbro with strongly zoned pyroxene grains up to 5 mm in length enclosing smaller subhedral laths of plagioclase (figure 3). Kushiro et al. (1972) reported small amount of olivine, both as subrounded phenocrysts and as fayalite located in the mesostasis (figure 4). The mesostasis includes chrome spinel, ilmenite, christobalite, troilite, phosphate, K-feldspar and K-Ba-rich residual glass.

El Goresy et al. (1972) and Haggerty (1972) found that 14053 was extremely reduced, with metallic iron in

Figure 2: Freshly sawn interior surface of 14053 showing basaltic texture. Cube is 1 cm. Photo # S75-33971.

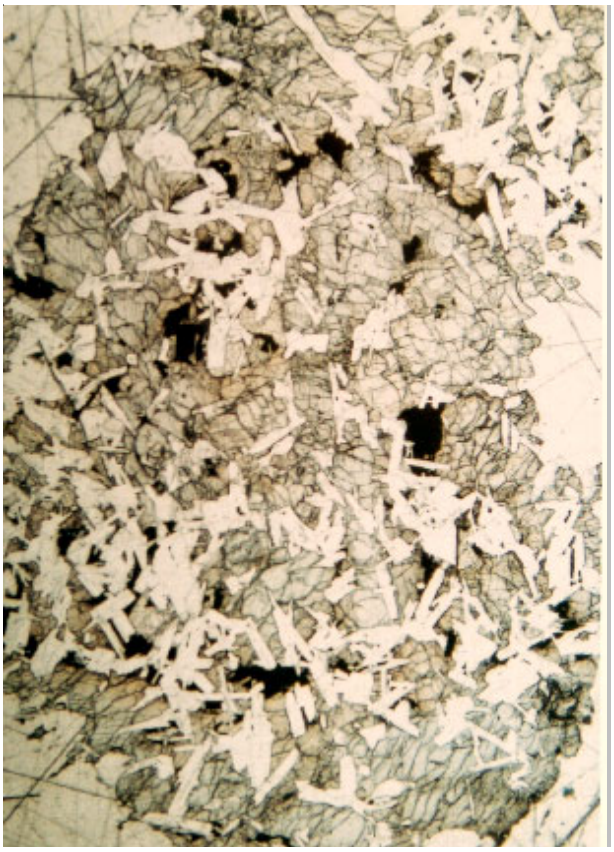

Figure 3: Thin section photomicrograph of 14053 showing ophitic texture. Photo # S71-23485. (Scale unknown, but probably ~3 mm top to bottom)

the mesostasis due to "subsolidus reduction." Patchen and Taylor (2004) have determined that the reduction is more pronounced in areas near the exterior of 14053, with both fayalite and ulvöspinel less reduced in the interior.

Mineralogy

Olivine: Fayalite is found intermixed with other accessory phases (SiO_2 etc) in the mesostasis (figure 6). Mayne and Taylor (2003) and Patchen and Taylor (2004) find that there is more breakdown by reduction of the fayalite near the exterior of 14053 than in the interior.

Pyroxene: Bence and Papike (1972) provide a large number of analyses of pyroxene in 14053, including minor element substitution. Schürmann and Hafner (1972) discuss the site occupancy of cations. Clinopyroxene zones all the way to heddenburgite and pyroxferroite (figure 4). Ghose et al. (1972) and Finger et al. (1972) also discuss pyroxene in 14053.

Mineralogical Mode

	Gancarz et al. 1971	Patchen and Taylor 2004	
		Interior	exterior
Plagioclase	50 % vol.	42	39
Pyroxene	40	48	48
Olivine		1.6	3.9
Ilmenite	3	2.3	4.3
Silica	2	2.4	2.6
Fayalite		0.9	0.3
Fe metal		0.09	0.3

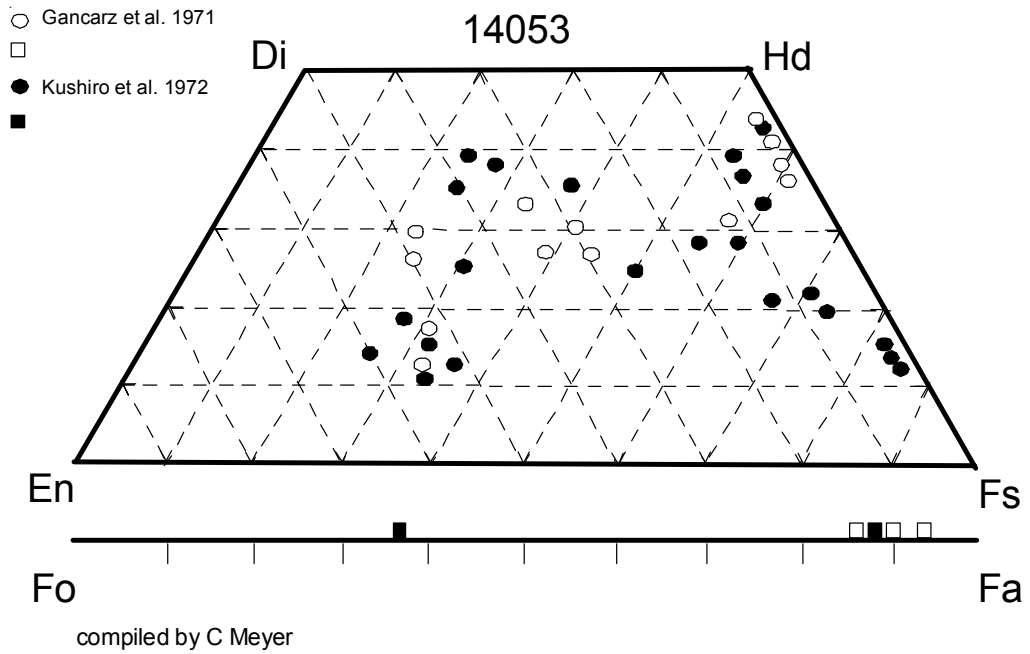

Figure 4: Composition diagram for pyroxene and olivine in 14053 (data replotted from Gancarz et al. 1971 and Kushiro et al. 1972 - see additional data in Bence and Papike 1975).

Plagioclase: The composition of plagioclase is relatively homogeneous (An_{91-93}) except near the rim (An_{70}) where it is found adjacent to K-feldspar (Kushiro et al. 1972). Wenk et al. (1972) and Czank et al. (1972) also studied plagioclase in 14053.

Opaques: Chrome spinel has been studied (Haggerty 1972, El Goresy et al. 1972, Mayne and Taylor 2003). Ulvöspinel is seen to break down by reduction to chrome spinel, ilmenite and Fe metal. Ilmenite has been analyzed (Garcarz et al. 1971). Metal grains in 14053 have high Ni, but lower than for other Apollo 14 basalts (Gancarz et al. 1971, El Goresy et al. 1972) (figure 5). The metal is found finely mixed with troilite in unique "spongy masses" (see picture in Gancarz et al. 1971).

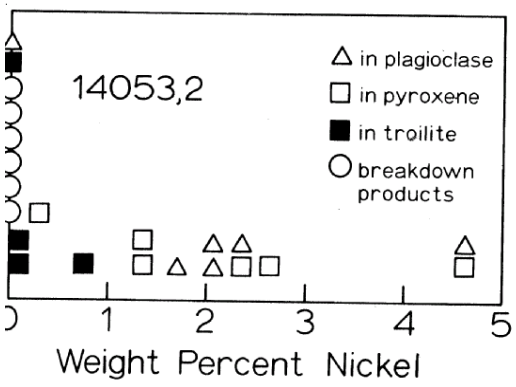

Figure 5: Ni content of metal grains in 14053 (from El Goresy et al. 1972).

Phosphates: Gancarz et al. (1971) analyzed apatite and whitlockite in 14053.

Glass: K and Ba-rich residual melt are found as glass in the mesostasis (El Goresy et al. 1972).

Chemistry

14053 has high Al content (table 1). Low siderophile elements were determined by Morgan et al. (1972). Figure 7 shows the REE.

Radiogenic age dating

14053 has been dated with good precision by Rb-Sr and Ar-Ar and appears to be older than the Fra Mauro Formation (see table and figures 8, 9).

However, in an effort to date the rock by Sm-Nd, Snyder and Taylor (2001) found that the Sm-Nd systematics were "disturbed". Tera and Wasserburg (1972) and Tatsumoto et al. (1972) determined the U-Th-Pb systematics of 14053 but could not obtain an age.

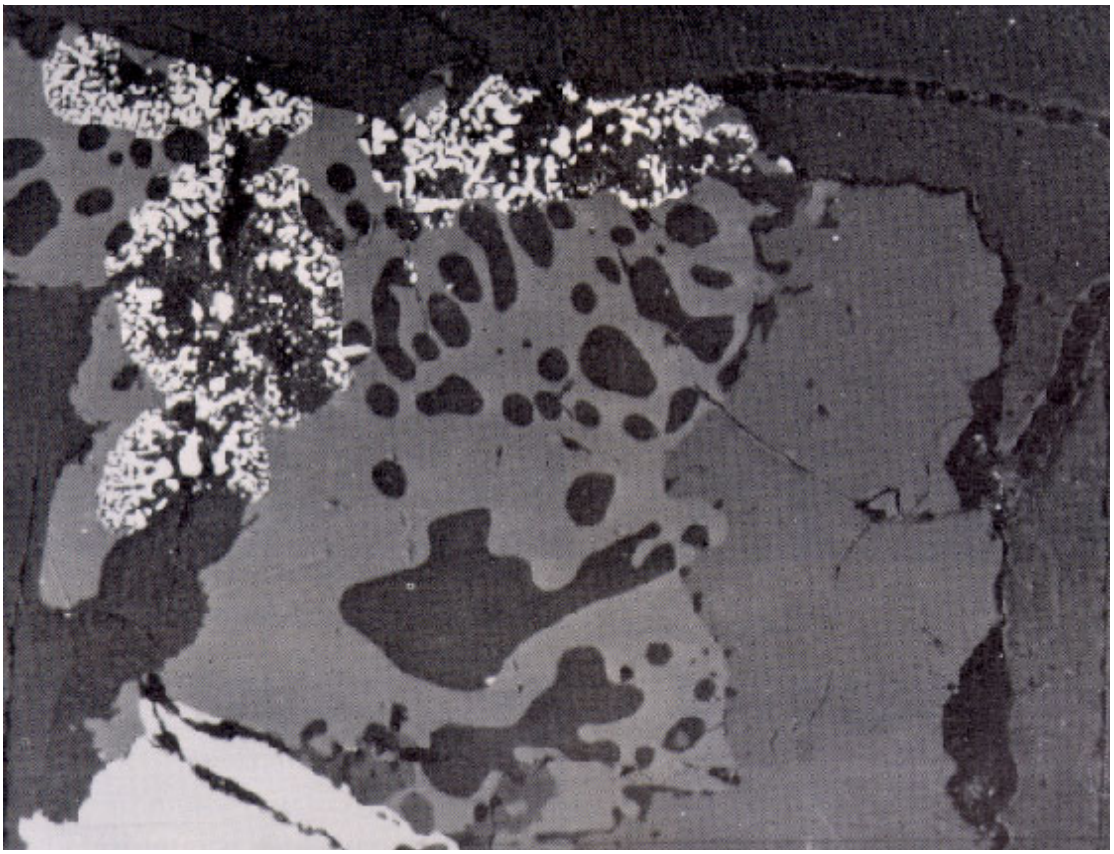

Figure 6: Reflected light photomicrograph of fayalite grain in process reduction to spongy Fe + silica (from El Goresy et al. 1971).

Cosmogenic isotopes and exposure ages

The ^{38}Ar exposure age (21 ± 5 m.y.) of 14053 is discussed in Husain et al. (1972). Eugster et al. (1984) determined an exposure age of 21.2 ± 5.0 m.y. by the ^{81}Kr method. This is interpreted to be the age of Cone Crater (Arvidson et al. 1975).

Other Studies

The composition of noble gasses in 14053 is given in Husain et al. (1972) and Eugster et al. (1984).

Processing

There are 21 thin sections of 14053.

List of Photo #s
S71-21353-357 B & W
S71-30464-495 B & W
S71-35849-854 Color
S72-34773-778 Nice color
S75-33968-973 Color saw cuts
S75-34136-138 Color

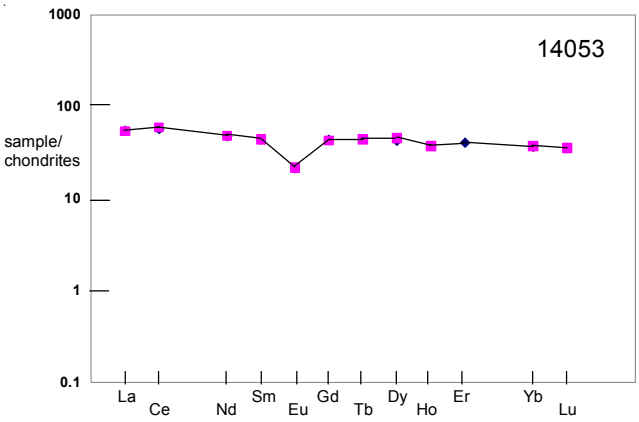

Figure 7: Normalized rare-earth-element diagram for 14053 (data from Hubbard et al. 1972 and Helmke et al. 1972).

Table 1. Chemical composition of 14053.

reference	*LSPET 71*		Willis 72		Helmke 72		Hubbard 72		Morgan 72		
weight											
SiO2 %	48	(c)	46.08	(a)			46.3	46.4	(a)		
TiO2	1.5	(c)	2.91	(a)			2.79	2.64	(a)		
Al2O3	12	(c)	12.54	(a)			13.7	13.6	(a)		
FeO	16	(c)	16.97	(a)			17	16.8	(a)		
MnO	0.29	(c)	0.255	(a)				0.26			
MgO	8.4	(c)	8.97	(a)			8.54	8.48	(a)		
CaO	12	(c)	11.07	(a)			11.2	11.2	(a)		
Na2O	0.38	(c)	0.44	(a)			0.44		(a)		
K2O	0.14	(c)	0.097	(a)			0.11	0.1	(a)		
P2O5			0.114	(a)			0.11	0.09	(a)		
S %			0.132	(a)				0.14			
sum											
Sc ppm	90	(c)			55	(b)					
V	135	(c)									
Cr	3000	(c)	2874	(a)							
Co	48	(c)									
Ni	14	(c)			14	(b)					
Cu	13	(c)									
Zn					3.4	(b)				2.1	(e)
Ga					4.8	(b)					
Ge ppb											
As											
Se											
Rb	2	(c)	2.2	(a)						2.1	(e)
Sr	180	(c)	98.6	(a)				98	(d)		
Y	90	(c)	54.7	(a)							
Zr	310	(c)	215	(a)							
Nb			15.7	(a)							
Mo											
Ru											
Rh											
Pd ppb											
Ag ppb										0.6	(e)
Cd ppb										20	(e)
In ppb											
Sn ppb											
Sb ppb										0.64	(e)
Te ppb										15	(e)
Cs ppm										0.09	(e)
Ba	190	(c)	163	(a)				146	(d)		
La	10	(c)			12.8	(b)		13	(d)		
Ce					36.4	(b)		34.5	(d)		
Pr											
Nd					22	(b)		21.9	(d)		
Sm					6.5	(b)		6.56	(d)		
Eu					1.23	(b)		1.21	(d)		
Gd					8.5	(b)		8.59	(d)		
Tb					1.62	(b)					
Dy					11.1	(b)		10.5	(d)		
Ho					2.1	(b)					
Er								6.51	(d)		
Tm											
Yb	10	(c)			6.1	(b)		6	(d)		
Lu					0.89	(b)					
Hf					9.8	(b)					
Ta											
W ppb											
Re ppb										0.007	(e)
Os ppb											
Ir ppb										0.017	(e)
Pt ppb											
Au ppb										0.11	(e)
Th ppm								1.63	(d)		
U ppm								0.6	(d)		

technique (a) XRF, (b) INAA, (c) emiss. Spec., (d) IDMS, (e) RNAA

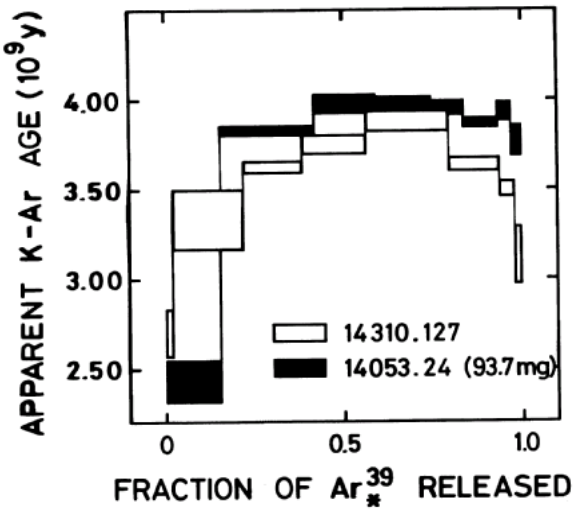

Figure 8: Ar plateau age of 14053 (from Stettler et al. 1973).

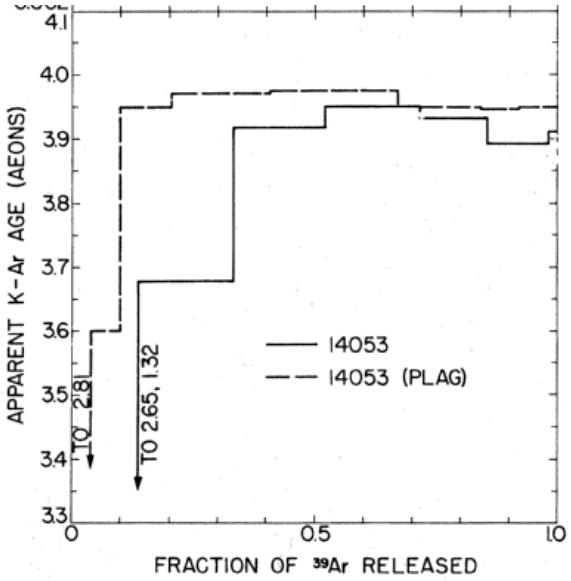

Figure 9: Ar plateau age of 14053 (from Turner et al. 1971).

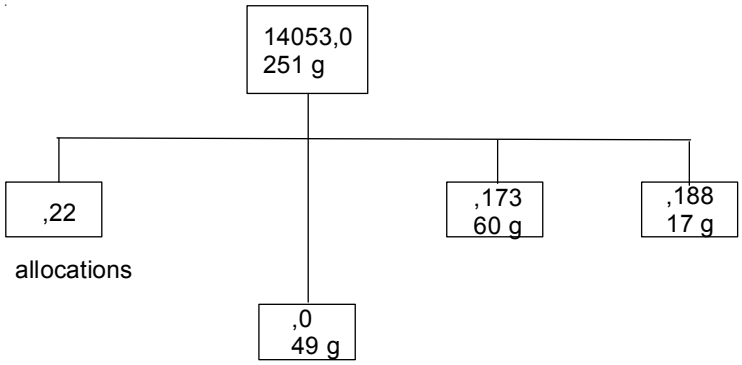

Summary of Age Data for 14053

	Rb-Sr	Ar plateau
Papanastassiou and Wasserburg 1971	3.96 ± 0.04	
Stettler et al. 1973		3.94 ± 0.04
Turner et al. 1971		3.94 ± 0.05
Husain et al. 1972		3.92 ± 0.08